Chemical Physics Letters 650 (2016) 148–153

Contents lists available at ScienceDirect

Chemical Physics Letters

journal homepage: www.elsevier.com/locate/cplett

Enhanced photothermal effect of surface oxidized silicon nanocrystals anchored to reduced graphene oxide nanosheets

Parichehr Afshani, Sherif Moussa, Garrett Atkinson, Vitaly Y. Kisurin, M. Samy El-Shall *

Department of Chemistry, Virginia Commonwealth University, Richmond, VA 23284, United States

ARTICLE INFO

Article history:
Received 25 November 2015
In final form 22 February 2016
Available online 2 March 2016

ABSTRACT

We demonstrate the coupling of the photothermal effects of silicon nanocrystals and graphene oxide (GO) dispersed in water. Using laser irradiation (532 nm or 355 nm) of suspended Si nanocrystals in an aqueous solution of GO, the synthesis of surface oxidized Si-reduced GO nanocomposites (SiO_x/Si-RGO) is reported. The laser reduction of GO is accompanied by surface oxidation of the Si nanocrystals resulting in the formation of the SiO_x/Si-RGO nanocomposites. The SiO_x/Si-RGO nanocomposites are proposed as promising materials for photothermal therapy and for the efficient conversion of solar energy into usable heat for a variety of thermal and thermomechanical applications.

Silicon nanostructures have been the subject of intense investigation for many years and the interest in the optical, photoluminescence and electrical properties of Si nanostructures continues to grow [1–4]. In addition to the size-dependent photoluminescence properties of Si nanocrystals and their use in display and optoelectronic applications, their high-capacity as anode materials for Li ion batteries, especially when coupled with graphene, has been recently demonstrated [5,6]. Furthermore, their biocompatible and biodegradable properties have triggered promising applications as in vivo imaging agents for a variety of applications in photothermal therapy and diagnosis [7–11].

Plasmonic nanoparticles such as gold, silver and copper have been the most extensively studied systems for photothermal therapy applications. For example, gold nanostructures with different sizes and shapes have been employed in photothermal therapeutics due to their strongly enhanced absorption in the visible and NIR regions caused by their surface plasmon resonance (SPR) oscillations [12–14].

In addition to gold nanoparticles, nanostructured carbon-based materials such as single wall carbon nanotubes, reduced graphene oxide (RGO) and GO have recently been applied in photothermal energy conversion as they can absorb light over extended regions of spectrum and convert it into heat through nonradiative decay processes [15–19]. The large surface area of graphene and RGO and the strong optical absorption across the spectrum coupled with its high thermal and chemical stability can lead to a rapid temperature rise and subsequent energy transfer to the host medium, thus offering an efficient way of heating the medium [20–23]. This has been demonstrated by the development of a facile laser reduction method for the synthesis of laser converted graphene (LCG) which provides a solution processable synthesis of individual graphene sheets [24,25]. In this process, irradiation of GO suspended in water using the second or the third harmonic of a Nd-YAG laser (532 nm or 355 nm, respectively) results in significant deoxygenation of GO and the formation of LCG. This remarkable photothermal conversion of energy results in a significant temperature rise of water from room temperature to 75 °C in a few minutes of laser irradiation (532 nm of nanosecond pulses at 30 Hz with an average power of 6 W) [24].

In this letter, we report enhanced photothermal effects with a new hybrid nanostructured material consisting of surface oxidized Si nanocrystals anchored to the surface of reduced GO nanosheets (SiO_x/Si-RGO). Hybrid materials composed of nanocarbons, such as the two-dimensional RGO, and semiconductor nanocrystals, such as silicon, could have important applications in photothermal therapy, solar cells, energy conversion and storing devices and nanoelectronics. Photothermal effects have been demonstrated for several semiconductor nanostructures such as Si nanowires [26], porous Si [27] and Ge nanocrystals [28]. Recently, a near-IR photothermal response of photoluminescent Si nanocrystals has been demonstrated [11]. However, there is no report on the photothermal energy conversion by surface oxidized Si nanocrystals anchored into RGO nanosheets. Here, we report on the laser surface oxidation of Si nanocrystals and the simultaneous reduction of GO to form surface oxidized Si-RGO nanocomposites (SiO_x/Si-RGO) as efficient photothermal agents for a variety of biomedical,

* Corresponding author.
E-mail address: mselshal@vcu.edu (M. Samy El-Shall).

http://dx.doi.org/10.1016/j.cplett.2016.02.056
0009-2614/

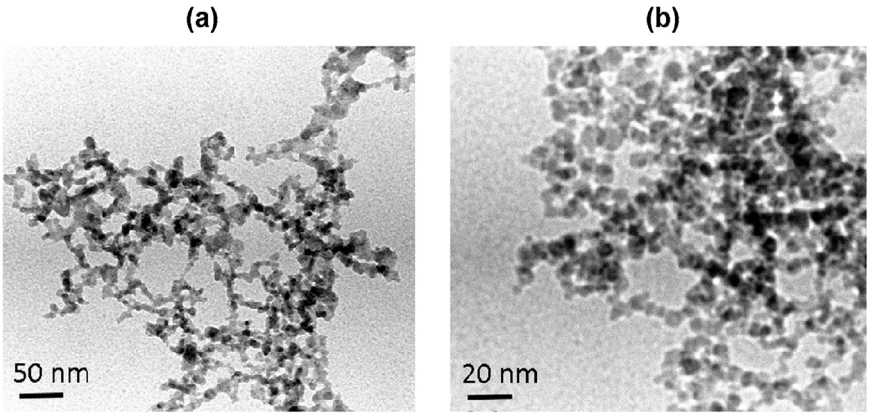

Figure 1. TEM images of Si nanocrystals prepared by the LVCC method using 500 Torr Ar (a), and 1000 Torr He (b).

thermal, thermochemical and thermomechanical applications. The availability of silicon, the second most abundant element in the Earth's crust, and the large production scale of graphite and GO coupled with the chemically inert nature of the SiO_x/Si-RGO nanocomposites could make these proposed applications economically attractive possibilities.

Si nanocrystals were prepared using the Laser Vaporization Controlled Condensation (LVCC) method [29–31]. The process consists of pulsed laser vaporization of a bulk Si target into an inert gas at well-defined temperatures and pressures inside a diffusion cloud chamber [29–31]. GO was prepared by the oxidation of high purity graphite powder (99.9999%, 200 mesh, Alfa Aesar) according to the method of Hummers and Offeman [32]. After repeated washing of the resulting yellowish-brown cake with hot water, the powder was dried at room temperature under vacuum overnight. For the laser irradiation and photothermal measurements [20], aqueous dispersions (3 ml) of GO (prepared using 2 mg solid GO in 10 ml deionized water) and preformed Si nanoparticles (1 mg or 2 mg Si nanoparticles in 3 ml GO dispersion or in 3 ml deionized water for blank experiments) were prepared and each dispersion (3 ml of either GO in water or Si nanoparticles in water or Si nanoparticles in the GO dispersion) was irradiated in a quartz cuvette with the unfocused beam of the second and third harmonics of a Nd:YAG laser (2nd harmonic $\lambda = 532$ nm, or 3rd harmonic $\lambda = 355$ nm, pulse width $\tau = 7$ ns, repetition rate = 30 Hz, fluence ~ 0.1 J/cm^2, Spectra Physics LAB-170-30). The beam diameter was measured to be 7–9 mm for both the 532 nm and 355 nm. The solutions were magnetically stirred during the irradiation (irradiation for 10 min corresponding to 18 000 laser shots). The temperature of the solution was monitored during the laser irradiation using a thermocouple immersed in the solution. The SiO_x/Si-RGO nanocomposite sheets were separated and dried overnight under vacuum before the XRD, Raman, IR and XPS measurements.

Figure 1 represents typical TEM images of the Si nanocrystals prepared by the LVCC method using Ar and He carrier gases [29–31]. The average sizes of the Si nanocrystals produced in 500 Torr Ar and 1000 Torr He are 5.5 nm and 4.5 nm, respectively. The particles formed in He are smaller since the lighter carrier gas is more effective in removing the small particles away from the nucleation zone in the LVCC chamber before they can grow into larger particles [29–31]. All the results reported below are obtained from the Si nanoparticles formed in 1000 Torr He.

The XRD pattern of the exfoliated GO (Figure S1(a), Supplementary material) [33] is characterized by a peak at $2\theta = 10.9^\circ$ with a larger d-spacing of 8.14 Å (compared to the typical value of 3.34 Å in graphite) resulting from the insertion of hydroxyl and epoxy groups between the carbon sheets and the carboxyl groups along the terminal and lateral sides of the sheets as a result of the oxidation process of graphite [24]. As shown in Figure S1(a), following the 532 nm or 355 nm laser irradiation in the presence of the Si nanocrystals, the $2\theta = 10.9^\circ$ completely disappears thus confirming the deoxygenation of the GO sheets and the restoration of the sp^2 carbon sites in the RGO nanosheets [24,25]. The 532 nm or 355 nm laser irradiation of GO in the presence of Si nanocrystals results in the disappearance of the $2\theta = 10.9^\circ$ diffraction peak similar to the laser irradiation of GO in the absence of Si nanoparticles [24]. However, the extent of the laser reduction of GO could be more enhanced by the presence of Si nanoparticles as demonstrated below. The XRD pattern of the Si nanoparticles with the characteristic diffractions 111, 220, and 311 at scattering angles of 28°, 47°, and 56°, respectively remains the same after the 355 nm or the 532 nm laser irradiation of the Si–GO solutions as shown in Figure S1(b), thus indicating the presence of Si nanoparticles within the RGO nanosheets.

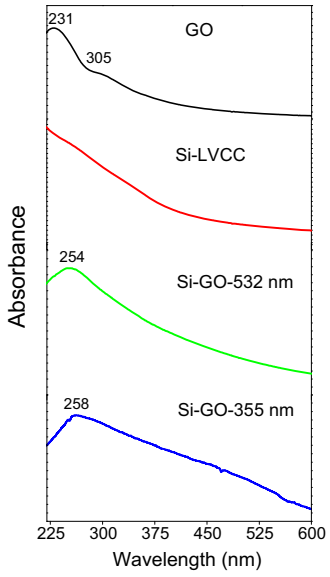

Figure 2. UV–vis absorption spectra of GO (2 mg solid GO in 10 ml water), Si nanoparticles prepared by the LVCC method (1 mg Si nanoparticles in 3 ml water), and Si nanoparticles–GO mixtures following laser irradiation using the 532 nm and 355 nm (1 mg Si nanoparticles in 3 ml GO dispersion above, 4 W laser power, 30 Hz, 10 min irradiation).

The UV–vis absorption spectrum of GO (displayed in Figure 2) shows significant absorption below 400 nm with the characteristic shoulder at 305 nm attributed to $n \rightarrow \pi^*$ transitions of C=O bonds [24,25]. This shoulder disappears after the 532 nm or the 355 nm irradiation of GO in the presence of Si nanocrystals as shown in